HHS Public Access

Author manuscript

Nat Neurosci. Author manuscript; available in PMC 2011 November 29.

Published in final edited form as:

Nat Neurosci. 2010 May ; 13(5): 584–591. doi:10.1038/nn.2535.

Selective induction of astrocytic gliosis generates deficits in neuronal inhibition

Pavel I. Ortinski[1,*], **Jinghui Dong**[2,*], **Alison Mungenast**[2], **Cuiyong Yue**[1], **Hajime Takano**[1], **Deborah J. Watson**[3], **Philip G. Haydon**[2], and **Douglas A. Coulter**[1,4]

[1]Division of Neurology, The Children's Hospital of Philadelphia, Philadelphia, PA

[2]Department of Neuroscience, Tufts University School of Medicine, Boston, MA

[3]Department of Neurosurgery, University of Pennsylvania School of Medicine, Philadelphia, PA

[4]Departments of Pediatrics and Neuroscience, University of Pennsylvania School of Medicine, Philadelphia, PA

Abstract

Reactive astrocytosis develops in many neurologic diseases including epilepsy. Astrocytotic contributions to pathophysiology are poorly understood. Studies examining this are confounded by comorbidities accompanying reactive astrocytosis. We found that high-titer AAV-eGFP astrocyte transduction induced reactive astrocytosis without altering the intrinsic properties or anatomy of neighboring neurons. We used selective astrocytosis induction to examine consequences on synaptic transmission in mouse CA1 pyramidal neurons. Neurons near eGFP-labeled reactive astrocytes exhibited reduction in inhibitory, but not excitatory synaptic currents. This IPSC erosion resulted from failure of the astrocytic glutamate-glutamine cycle. Reactive astrocytes downregulated expression of glutamine synthetase. Blockade of this enzyme normally induces rapid synaptic GABA depletion. In astrocytotic regions, residual inhibition lost sensitivity to glutamine synthetase blockade, while exogenous glutamine administration enhanced IPSCs. Astrocytosis-mediated deficits in inhibition triggered glutamine-reversible hyperexcitability in hippocampal circuits. Reactive astrocytosis may thus generate local synaptic perturbations, leading to broader functional deficits associated with neurologic disease.

Keywords

adeno-associated virus; reactive astrocytes; glia; synaptic transmission; inhibitory; glutamate-glutamine cycle; hippocampus; patch-clamp

Corresponding Author: Douglas A. Coulter, Ph.D. Children's Hospital of Philadelphia, Abramson Research Center, Room 410 D, 3615 Civic Center Boulevard, Philadelphia, PA 19104-4318. coulterd@email.chop.edu.

*JD and PIO contributed equally to this work.

AUTHOR CONTRIBUTIONS

PIO and JD conducted and analyzed all of the experiments. AM assisted with viral vector production. CY contributed to VSD data collection and analysis. HT assisted with confocal data acquisition and processing. DJW contributed to initial generation of the AAV-injected mice. PIO and DAC wrote the manuscript with help from PGH and JD. DAC and PGH designed the experiments with PIO and JD and supervised the project.

Astrocytes regulate synaptic function throughout the brain[1–3]. One notable aspect of this is the role these cells play in neurotransmitter recycling. Following synaptic release, glia restrict diffusion, sequester, inactivate and recycle a variety of small molecule neurotransmitters including glutamate, GABA, and catecholamines[4–6]. In the case of glutamate and GABA, the keystone astrocytic enzyme regulating recycling is glutamine synthetase, which produces glutamine from glutamate following glial uptake of this neurotransmitter. Glutamine is transported back to presynaptic terminals via glia- and neuron-specific glutamine transporters, and converted to glutamate by the mitochondrial enzyme, glutaminase[4,7], to be reused in synaptic function either directly or following conversion to GABA.

This multi-cellular enzymatic process, termed the glutamate-glutamine cycle, is critical in maintaining ongoing synaptic function. Inhibitory synapses fail following disruption of the glutamine cycle[8,9], while excitatory synapses have sufficient reserve glutamate to transiently retain function[10]. In various CNS disease states, including epilepsy, Parkinson's disease, Alzheimer's disease, stroke and traumatic brain injury, there is growing evidence for compromised function of the glutamate-glutamine cycle[11–16]. All of these pathologic conditions are also associated with the development of astrocytic alterations, termed reactive astrocytosis.

Reactive astrocytosis is defined and characterized by gross hypertrophy of the cell body and processes of astrocytes in injured and/or diseased areas of the brain[17]. Accompanying these anatomic changes is enhanced expression of glial cytoskeletal proteins, glial fibrillary acidic protein (GFAP) and vimentin[17,18]. Enhanced expression of these two proteins is therefore of diagnostic utility in assessing the development of reactive gliosis. The disease in which reactive astrocytosis has arguably received the most experimental attention is temporal lobe epilepsy (TLE)[19]. The pathological hallmark of TLE is mesial temporal sclerosis, defined as segmental neuronal loss and reactive astrocytosis in the hippocampus and associated temporal lobe structures.

In TLE, a series of phenotypic changes accompany cell hypertrophy in reactive astrocytes. Notable among these are reductions in expression of proteins critical in function of the glutamine cycle, including glutamine synthetase and the astrocytic glutamate uptake transporters, EAAT1 and EAAT2[11–13] (but see[20]). Recognition of the pivotal role that these proteins play in neurotransmitter uptake and recycling has led to the hypothesis that glutamine cycle deficits associated with the development of reactive astrocytosis may be contributing to the epilepsy disease phenotype[8,12,19]. However, studies attempting to critically assess this hypothesis have been limited by the broad constellation of structural and functional changes evident in the hippocampi of patients with TLE and also in animal models of epilepsy.

In the present study, we made use of the observation that high-titer viral transduction of astrocytes led to selective virus-induced reactive astrocytosis in the absence of alterations in adjacent neurons and microglia. Using this model, we assessed the effects of virus-induced reactive astrocytosis on synaptic transmission in hippocampal area CA1. We found that astrocytosis induces specific deficits in inhibitory synaptic transmission precipitating

disruptions in functional regulation of circuits consistent with enhanced excitability. This could contribute to elevated seizure susceptibility underlying TLE.

RESULTS

Viral induction of reactive astrocytosis

We evaluated transduction patterns of six adeno-associated virus (AAV) pseudotypes: AAV2/1, 2/2, 2/5, 2/7, 2/8, and 2/9. Of these six, AAV2/1, AAV2/5, AAV2/7, and AAV2/9 were the most effective in inducing CMV promoter-driven eGFP expression in the hippocampus (Fig. S1). AAV2/9 showed preferential neuronal tropism while AAV2/5 predominantly labeled astrocytes, displaying robust co-localization of eGFP with the astrocytic marker, GFAP (85%, Fig. S1, S2). Substitution of the CMV with a GFAP promoter (gfa104) increased astrocyte-specific expression to >99% (Fig. 1). We observed no co-localization of AAV2/5 eGFP with NG2-positive oligodendrocyte progenitors, mature oligodendrocytes, or microglia (Fig. S3), again indicating preferential tropism of AAV2/5 for astrocytes. AAV2/5-transduced astrocytes were characterized by a viral titer-dependent cellular hypertrophy, consistent with their activation by the virus (Fig. 1e–g, Fig. 2). Bromodeoxyuridine (BrdU) administered for 1 week during development of astrogliosis labeled only 1% of eGFP/GFAP positive astrocytes, indicating that virally-induced hypertrophy occurred in the absence of hyperplasia. Up-regulation of GFAP and vimentin are two of the most prominent biochemical markers of astrocyte reactivity[17]. The expression levels of both these proteins significantly increased in the hippocampus following injection of the high (3×10^{10} genome copies (GC)/injection), but not the lower (1×10^{9} GC/injection) titer of AAV2/5-gfa104-eGFP (Fig. 2a–h,q,r). Reactive astrocytosis was induced locally, in the absence of microglial reactivity (Fig. S4). Furthermore, high-titer AAV2/9 did not induce reactive astrocytosis, demonstrating that astrocyte activation was not an inflammatory response to intrahippocampal injection of virus or to neuronal transduction (Fig. S5).

Several studies have implicated reduced glutamine synthetase levels associated with the development of astrocytosis in the pathophysiology of epilepsy[11,12,21]. Consistent with these findings, we observed a pronounced down-regulation of glutamine synthetase expression following injection of high-titer AAV2/5 (Fig. 2i–p,s), but not of the equivalent AAV2/9 titer (Fig. S5g). This was also associated with enhanced GFAP and vimentin expression (Fig. 2, Fig. S6). Since astrocytic glutamine synthetase is the primary enzyme generating glutamine in the brain, these results suggested that development of reactive astrocytosis will disrupt neuronal glutamine supply and should generate a deficit in inhibitory neurotransmission in neurons located in areas populated by reactive astrocytes ($eGFP^{+}$ areas).

Basal and dynamic failure of IPSCs in astrocytotic regions

To evaluate the consequences of reactive gliosis on synaptic efficacy, we began by recording monosynaptic inhibitory responses (eIPSCs) in CA1 pyramidal neurons, elicited by local interneuron stimulation. eIPSCs in neurons located within $eGFP^{+}$ areas were markedly smaller than eIPSCs recorded both in neurons from control animals and in neurons

located in eGFP$^-$ areas of AAV2/5-treated animals (Fig. 3a). The amplitude distribution of eIPSCs in cells from eGFP$^+$ areas was skewed toward small amplitude events (skewness=1.15±0.51, p=0.002, K-S test) and was significantly different from the control cell population (p=0.013, K-S test) with the low amplitude (<50 pA) component accounting for 55% of all responses (Fig. 3b). Distributions of eIPSC amplitudes recorded from neurons in naïve animals, animals injected with AAV2/9, and eGFP$^-$ areas of AAV2/5-injected animals were not significantly different (average eIPSC in naïve: 91.74±12.62 pA, n=11; AAV2/9: 99.9±12 pA, n=8; eGFP$^-$: 87±15, n=7) and were pooled for analysis (Fig. 3b). The eIPSC amplitude distribution in this composite control group of cells was normal (skewness=0.46±0.46, p=0.2, K-S test) with the majority of eIPSCs in the 51–100 pA range. In a series of control experiments, we injected animals with a low titer AAV2/5 (1×10^9 GC/injection), which does not induce reactive astrocytosis (Fig. 2). The frequencies of low (<50 pA) and high (>50 pA) amplitude events in pyramidal cells from low titer AAV2/5 eGFP$^+$ areas did not differ from the respective frequencies in cells from control animals (p=0.37, n=12, binomial test, no overall difference in amplitude distributions p=0.3, K-S test, Fig. S7). Additionally, paired pulse ratios were similar between cells from high-titer AAV2/5 eGFP$^+$ areas and control cells, consistent with similar initial probability of release at GABAergic synapses onto both groups of cells (control PPR=0.51±0.02, n=4, AAV2/5 PPR=0.55±0.06, n=5, p=0.56).

We next investigated quantal post-synaptic responses by recording spontaneous, miniature IPSCs (mIPSCs) in the presence of tetrodotoxin and glutamatergic antagonists. The amplitude distribution of mIPSCs recorded from neurons in eGFP$^+$ regions was left-shifted relative to controls (Fig. 3c,d). mIPSC frequency was also reduced by 35% in neurons from eGFP$^+$ regions (AAV2/5: 10.3±1.8 Hz; control: 15.8±1.4 Hz, p=0.04), likely due to a subset of small events in AAV2/5 cells falling below the noise threshold. There was no difference in mIPSC decay time kinetics between the two groups (AAV2/5: τ_w=6.3±1.1 ms; control: τ_w=6.4±1.1 ms). These data support the observation that neurons within regions of astrocytic reactivity exhibit a significant basal deficit of inhibitory neurotransmission. Moreover, preferential impairment of small, but not large amplitude mIPSCs is consistent with a pre-synaptic origin of this deficit[22] (see Discussion).

To evaluate inhibitory synaptic function in pyramidal neurons under conditions of sustained activation similar to that exhibited in vivo, we recorded eIPSCs generated by a long duration stimulus train. The train consisted of 50 Hz bursts of 4 pulses, every 20 s for 15 min. In control cells, eIPSC amplitudes significantly increased during the train (204±16% of pre-train values, n=10, p=0.004, paired t-test), but returned to pre-train values following train stimulation (102±8%, Fig. 3e). In contrast, eIPSC amplitudes in neurons within eGFP$^+$ areas (c.f. Fig. 3f) were not enhanced during the train (96.5±8.7% of pre-train values, n=10), and, following the train stimulation, decreased to 57.5±9.4% of pre-train values (Fig. 3e, p=0.003 compared to controls).

Astrocytes release a number of molecules to modify neuronal activity, including ATP[2] and glutamate[23]. To assess whether modifications in astrocytic release accompanying viral-induced reactivity could account for the failure of inhibition described above, we blocked neuronal receptors for these gliotransmitters. In slices from AAV2/5 animals, addition of

purine (P2), adenosine (A1), and mGluR II/III antagonists (PPADS (50 μM), DCPX (800 nM), and CPPG (300 μM), respectively) did not significantly alter the amplitude or charge transfer of eIPSCs or eEPSCs relative to responses evoked in the absence of these drugs (in the presence of antagonists: eIPSC amplitude: 48.2±9.4, n=6, p=0.121, eIPSC charge: 2.45±0.61, n=6, p=0.174; eEPSC amplitude: −154.8±70 pA, n=4, p=0.168, eEPSC charge: 0.54±0.27, n=4, p=0.5).

Excitatory signaling is unaltered by virus-induced astrocytosis

We next examined excitatory postsynaptic currents (eEPSCs) in areas exhibiting reactive astrocytosis. Compound synaptic responses were recorded in the absence of glutamate and $GABA_A$ receptor antagonists. Under these conditions, eIPSCs could be seen to follow eEPSCs arising from activation of Schaffer collateral synapses on pyramidal cell dendrites (Fig. 4a). eEPSC amplitude and charge in cells in $eGFP^+$ areas were not significantly different from control cells (Fig. 4b). In the same compound EPSC/IPSC recordings, IPSC amplitude and charge were significantly depressed in neurons adjacent to AAV2/5 $eGFP^+$ cells compared to controls (Fig. 4c), similar to the 55% of $eGFP^+$ neurons with small eIPSCs evident in monosynaptic recordings (Fig. 3b).

We then investigated eEPSCs using stimulation protocols designed to interrogate the dynamics of vesicle pool release and recovery. Two synaptic vesicle populations respond to electrical stimulation: a readily-releasable pool (RRP), comprised of docked, active zone vesicles available for immediate release, and a reserve pool, representing the vesicles drawn upon when the RRP is depleted[24]. Release from the RRP can be triggered by brief electrical stimulation, while release from reserve pool requires prolonged stimulation protocols[25]. Using these published stimulation parameters and in the presence of picrotoxin (100 μM) and D-AP5 (50 μM), we found that recovery from stimulation-induced depletion of the RRP and the reserve pool of vesicles at excitatory synapses occurred with a similar time course in both AAV2/5 and control neurons (Fig. 4d–f). However, *during* both RRP and reserve pool stimulations, facilitation of eEPSCs was stronger in control neurons than in AAV2/5 cells (Fig. S8), implicating differences in short-term plasticity.

Taken together, these results indicate that virus-induced reactive astrocytosis leads to a broad impairment of inhibitory, but not excitatory neurotransmission.

Astrocytosis does not affect neuronal membrane properties

CA1 pyramidal neurons located in $eGFP^+$ areas were indistinguishable from neurons in naïve animals across a number of membrane property measures (Supplementary Table 1, Fig. S9). Furthermore, intracellular labeling of control (n=9) and AAV2/5 (n=8) cells confirmed preservation of pyramidal cell morphology, dendritic arborization and dense investiture of astrocytic processes adjacent to label-filled soma and neurites (Fig. S10). These results indicated that CA1 pyramidal neurons remained structurally and functionally viable and that their intrinsic properties were not altered by local astrocytosis.

Changes in inhibitory synaptic strength in $eGFP^+$ areas of AAV2/5-treated animals could be generated by altered excitability of local interneurons. Multiple subtypes of hippocampal

interneurons targeting pyramidal cell dendrites have been identified. We examined the somatostatin-containing O-LM interneurons selectively labeled by eGFP in a transgenic mouse line, GIN[26]. Interneuron phenotype was verified anatomically (by GFP and Alexa 594 fluorescence) and physiologically, by lack of action potential accommodation.. We found no differences in seven basic electrophysiological parameters between six control neurons and five neurons in $eGFP^+$ areas of AAV2/5 slices (Supplementary Table 2, Fig. S11), indicating that interneurons are unlikely to contribute to the inhibitory deficit observed in pyramidal cells in $eGFP^+$ areas.

Astrocytosis-induced glu/gln cycle compromise impairs inhibition

Astrocytic glutamine maintains inhibitory efficacy in CA1 pyramidal cells, and blockade of glutamine synthetase precipitates activity-dependent failure of eIPSCs[8]. In control cells, blocking glutamine synthetase activity with methionine sulfoximine (MSO), decreased eIPSC amplitudes during and following the train stimulation to 50±7% and 47±6% of MSO-free responses, respectively (n=8, Fig. 5a). $eGFP^+$ reactive astrocytes from high titer AAV2/5 animals exhibit a pronounced down-regulation of glutamine synthetase expression (Fig. 2i–l and Fig. S6), which should occlude the effects of MSO on eIPSCs. Indeed, MSO treatment had no effect on eIPSCs recorded in CA1 neurons in $eGFP^+$ areas. eIPSC amplitudes in these cells during and following the train were 98±12% and 107±17% of MSO-free responses, respectively (n=9, compare Fig. 5a to Fig. 3e).

Decreased glutamine synthetase activity will deplete glutamine available for neuronal uptake. Since glutamine is converted to glutamate and then to GABA in inhibitory nerve terminals, glutamine deficiency reduces the pool of GABA available for synaptic release. We confirmed reduction in synaptic GABA by recording mIPSCs in the presence of 1,2,5,6-tetrahydropyridine-4-yl)methylphosphinic acid (TPMPA), a low affinity $GABA_A$ antagonist with a fast unbinding rate. Lower levels of synaptic GABA will result in a briefer synaptic cleft transient of GABA, and a larger suppression of mIPSCs amplitude by TPMPA[8,22]. Consistent with this prediction, TPMPA (30 μM) produced minimal effect in neurons from control slices (98.9±8.5%, n=6), but decreased mIPSC amplitude to 74.6±4.2% of baseline in neurons from AAV2/5-injected animals (n=6, p=0.027). In contrast, a high-affinity, $GABA_A$ antagonist, SR-95531 (300 nM), blocked mIPSCs equivalently in AAV2/5 and control groups (AAV2.5: 81.5±5.4%, n=5; control: 81.7±3.3%, n=6, p=0.97, Fig. 5b).

If neuronal glutamine starvation mediates eIPSC failure, eIPSCs should be rescued by exogenous glutamine. Bath application of glutamine (10 mM) increased eIPSC amplitude to 126±6% of pre-treatment levels in 7 out of 11 CA1 neurons in $eGFP^+$ areas of AAV2/5 slices. Glutamine had no effect in control neurons (91±4%, n=7, Fig. 5c, group effects differ, $p<0.001$). Glutamine application also attenuated the dynamic failure of eIPSCs following train stimulation (Fig. 5c *right*) to 88.6±8.6% of pre-train baseline (n=5, p=0.04 relative to AAV2/5 neurons in the absence of glutamine), but failed to reverse the reduction of eIPSC amplitudes during the train (Fig. 5c *right*). The latter may suggest gliosis-triggered recruitment of glutamine cycle-independent mechanisms modulating short-term synaptic plasticity (see Discussion).

These results indicate that reactive astrocytosis-induced glutamine synthetase reduction leads to interrupted neuronal glutamine supply, impaired neuronal production of GABA, and compromised inhibitory neurotransmission.

Virus-induced astrocytosis alters network excitability

To evaluate whether the inhibitory deficits observed at a cellular level translate into altered network function, we examined CA1 circuit activity triggered by temporoammonic pathway (TAP) stimulation, using voltage-sensitive-dye (VSD) imaging techniques. TAP activation of CA1 network responses is strongly regulated by feedforward inhibition, which constrains EPSPs to distal dendrites of CA1 pyramidal cells[27,28]. Loss of inhibitory control over TAP signaling following induction of astrogliosis should result in a more powerful excitation similar to that observed in slices from epileptic animals[28]. Following TAP stimulation, we recorded sustained EPSPs propagating to *stratum radiatum* and *stratum oriens* in 63% (10 out of 16) of $eGFP^+$ slices from 5 animals. In 6 out of 6 control slices, EPSPs propagated only to distal *stratum radiatum* and elicited an IPSP in *stratum oriens* of area CA1 (Fig. 6a–c). In *stratum oriens*, IPSPs observed in control slices converted to EPSPs in astrogliotic slices (control dF/F: −0.024±0.005%, n=6; AAV2/5 dF/F: 0.064±0.014%, n=10, $p<0.001$, Fig. 6d). This was accompanied by a 20-fold increase in area activated by TAP stimulation in the AAV2/5 group ($p<0.002$, Fig. 6e). Whole-cell current-clamp recordings from CA1 pyramidal neurons confirmed that TAP activation triggers an EPSP in neurons located proximal to reactive astrocytes, and an IPSP in control neurons (Fig. 6c **bottom row**, controls: −2.7±0.8 mV, n=3; AAV2/5: 2.1±0.5 mV, n=6).

We examined whether exogenous glutamine would reverse the circuit hyperexcitability associated with reactive gliosis. In $eGFP^+$ slices, application of 10 mM glutamine reduced the *stratum radiatum* and *stratum oriens* EPSPs to 64±14% and 43±15% of pre-glutamine levels (n=5, no effect in 1 slice, Fig. 6f,g) and similarly reduced the activated areas (*radiatum*: 68±20%, *oriens*: 47±15% of pre-glutamine levels (Fig. 6h).

Thus, inhibitory deficits associated with reactive gliosis lead to hyperexcitability of the hippocampal network, and this can be partially ameliorated by exogenously supplied glutamine.

DISCUSSION

Virus-induced reactive astrocytosis triggered a selective deficit in inhibitory synaptic transmission in hippocampal neurons. This occurred in the absence of potentially confounding pathophysiologic effects of brain injury and/or inflammation, which usually accompany the development of astrocytosis. Impaired inhibitory neurotransmission was due to a disruption of the astrocytic glutamate/glutamine cycle, mediated by glutamine synthetase downregulation in reactive astrocytes. This led to reduced availability of glutamine for neuronal uptake and concomitant reduced synaptic GABA availability. The compromised glutamate/glutamine cycle function and associated failure of inhibition resulted in network hyperexcitability similar to that seen in animal models of TLE[28].

Specific association of astrocytosis and synaptic deficits

The mechanism underlying virus-induced reactive astrocytosis is not known. Two possibilities include capsid interactions with cellular receptors that lead to preferential viral transduction or the result of viral DNA interacting with toll-like receptors. Regardless of mechanism, our data are consistent with an astrocytic basis for reactivity. When using AAV2/9, which selectively transduces neurons, reactive astrocytosis was not detected. Thus, it is the interaction of the virus with the astrocyte that is important for the resulting reactive astrocytosis. When we performed experiments using AAV2/5 and the CMV promoter we never detected expression in microglia (unpublished observation), thus we can discount this cell type as contributing to the process. There is a remote possibility that the few neurons that can be transduced by AAV2/5 would have led to reactive astrocytosis. However, if this were the case we would expect the neurons to also affect the microglia. We did not detect a stimulation of CD45 staining of microglia and therefore feel such a scenario is not likely.

The use of AAV as a selective tool to generate reactive astrocytosis isolated from other pathologic processes allowed us to determine whether changes in synaptic transmission specifically accompany astrocytic reactivity. We observed reduced expression of glutamine synthetase in astrocytes as well as a correlated reduction in inhibitory transmission. In two tests of a causal relationship, the effects of glutamine cycle antagonists on inhibitory function were occluded in regions of reactive gliosis, and exogenous glutamine led to a partial recovery of synaptic function. Since glutamine is selectively synthesized in astrocytes, these results support our conclusion that reactive astrocytosis leads to impaired inhibitory synaptic transmission as a consequence of reduced glutamine synthetase expression and glutamine supply. Additionally, we demonstrate that astrocytosis leads to changes in network excitability, which can be attenuated by exogenous glutamine (Fig. 6).

Astrocytosis-triggered IPSC failure

Several variables must be considered when interpreting the potential effects of virally-induced reactive gliosis on inhibition. First, there are multiple vesicle populations in inhibitory terminals, including the readily releasable and recycling pools that were sampled in our studies. GABA content in these distinct pools may derive from differing sources, and so exhibit differential sensitivity to gliosis. Second, the viral strategy activates many, but not all astrocytes, and, since astrocytes occupy non-overlapping synaptic territories[29], some of neuron's inhibitory synapses may be invested into by reactive astrocytes and some by remaining unaffected astrocytes. This could contribute to variation in the degree of effect of gliosis on small vs. large amplitude IPSCs.

Assuming that postsynaptic receptors are unchanged, we hypothesize that deficits in pre-synaptic GABA levels will be predominantly evident during IPSCs elicited by non-saturating neurotransmitter concentrations, i.e. small amplitude events. At these synapses, neurotransmitter concentration determines IPSC amplitude and gliosis-induced decrease in synaptic GABA directly translates to smaller responses. In contrast, at synapses which function in a suprasaturated state, a fractional reduction in vesicular GABA due to gliosis might still be sufficient to fully occupy postsynaptic receptors (i.e. receptor availability, not neurotransmitter concentration, is rate-limiting) Thus, large amplitude events would tend to

be less affected than small amplitude events. Our data are consistent with these predictions and are bolstered by examination of quantal synaptic events, mIPSCs. In AAV2/5 neurons, the mIPSC amplitude distribution is left-shifted due to increased contribution of small amplitude events. In addition, the fast-off, low-affinity $GABA_A$ antagonist, TPMPA, is more effective in AAV2/5 compared to control neurons, while the high-affinity $GABA_A$ antagonist, SR95531, is equally effective in both groups of neurons. Both of these effects would be expected from reduced GABA levels in a population of synapses or in a subset of synaptic vesicles[22,30,31].

Lack of effect of virus-induced astrocytosis on EPSCs

Preservation of EPSCs in cells proximal to reactive astrocytes exhibiting glutamine synthetase down-regulation corroborates a recent study demonstrating that excitatory signaling is not affected by glutamate/glutamine cycle inhibitors[10]. Together with our results, these data suggest that GABAergic signaling relies on astrocyte-derived glutamine to a greater extent than glutamatergic synapses, which may depend more on direct uptake of glutamate into neurons, and/or have a higher basal cytoplasmic reserve of this amino acid than interneurons.

We observed no differences in excitatory drive onto CA1 pyramidal cells following stimulation of the RRP and the reserve pool of vesicles. However, pyramidal cells neighboring reactive astrocytes showed reduced short-term facilitation of eEPSCs during the RRP and the early stage of the reserve pool trains (Fig. S8) suggesting higher initial release probability of glutamate-containing vesicles[32]. Interestingly, a similar alteration in short term plasticity was evident for IPSCs. In cells from $eGFP^+$ slices, train-induced eIPSC facilitation (Fig. 3e) was reduced and this was not rescued by exogenous glutamine (Fig. 5c *right*). These findings indicate that development of astrocytosis alters both excitatory and inhibitory short-term synaptic plasticity through mechanisms independent of the astrocyte-derived glutamine.

Experimental astrocytosis accompanied by brain inflammation has been induced by systemic injection of the bacterial endotoxin, lipopolysaccharide (LPS). This *increases* both excitatory and inhibitory drive in the hippocampus[33,34]. LPS triggers both inflammation and astrocytosis, unlike AAV2/5-induced astrocyte reactivity, which generated astrocytosis in the absence of microglial activation. Moreover, LPS effects are distributed broadly throughout the brain, while AAV2/5 is relatively local. This underscores the importance of distinguishing between neuronal deficits precipitated by a global brain pathology accompanied by inflammation and those specifically associated with local glial reactivity.

Conclusion

Reactive astrocytes are associated with many disease and injury states, and have been implicated in the maintenance of epileptic seizure foci[16,35]. Our studies demonstrate a specific association of virus-induced reactive astrocytosis with a deficit of inhibitory, but not excitatory neurotransmission. The inhibitory deficit is spatially restricted to areas of high astrocytic reactivity and is precipitated by decreased synthesis of glutamine in astrocytes. By starving inhibitory synapses of the GABA precursor, glutamine, reactive astrocytes exert

powerful control over the efficacy of GABAergic synapses. Given the critical importance of GABAergic inhibition in neuronal circuit regulation, the altered role reactive astrocytes play in regulating synaptic function is likely to have significant functional consequences in CNS disease states associated with astrocytosis, potentially eroding many emergent functions of neuronal circuits, such as cognition, learning and memory, movement generation and coordination, and resistance to seizure generation.

Supplementary Material

Refer to Web version on PubMed Central for supplementary material.

Acknowledgments

Supported by P01 NS054900 and P20 MH071705 to DAC, by the Epilepsy Foundation Fellowship to PIO, and by P01NS054900 RO1NS054770, and RO1NS037585 to PGH.

References

1. Haydon PG, Carmignoto G. Astrocyte control of synaptic transmission and neurovascular coupling. Physiol Rev. 2006; 86:1009–31. [PubMed: 16816144]
2. Pascual O, Casper KB, Kubera C, Zhang J, Revilla-Sanchez R, Sul JY, Takano H, Moss SJ, McCarthy K, Haydon PG. Astrocytic purinergic signaling coordinates synaptic networks. Science. 2005; 310:113–6. [PubMed: 16210541]
3. Volterra A, Meldolesi J. Astrocytes, from brain glue to communication elements: the revolution continues. Nat Rev Neurosci. 2005; 6:626–40. [PubMed: 16025096]
4. Bak LK, Schousboe A, Waagepetersen HS. The glutamate/GABA-glutamine cycle: aspects of transport, neurotransmitter homeostasis and ammonia transfer. J Neurochem. 2006; 98:641–53. [PubMed: 16787421]
5. de Melo Reis RA, Ventura AL, Schitine CS, de Mello MC, de Mello FG. Müller glia as an active compartment modulating nervous activity in the vertebrate retina: neurotransmitters and trophic factors. Neurochem Res. 2008; 33:1466–74. [PubMed: 18273703]
6. Syková E, Nicholson C. Diffusion in brain extracellular space. Physiol Rev. 2008; 88:1277–340. [PubMed: 18923183]
7. Chaudhry FA, Reimer RJ, Edwards RH. The glutamine commute: take the N line and transfer to the A. J Cell Biol. 2002; 157:349–55. [PubMed: 11980913]
8. Liang SL, Carlson GC, Coulter DA. Dynamic regulation of synaptic GABA release by the glutamate-glutamine cycle in hippocampal area CA1. J Neurosci. 2006; 26:8537–48. [PubMed: 16914680]
9. Fricke MN, Jones-Davis DM, Mathews GC. Glutamine uptake by System A transporters maintains neurotransmitter GABA synthesis and inhibitory synaptic transmission. J Neurochem. 2007; 102:1895–904. [PubMed: 17504265]
10. Kam K, Nicoll R. Excitatory synaptic transmission persists independently of the glutamate-glutamine cycle. J Neurosci. 2007; 27:9192–200. [PubMed: 17715355]
11. Eid T, Thomas MJ, Spencer DD, Runden-Pran E, Lai JC, Malthankar GV, Kim JH, Danbolt NC, Ottersen OP, de Lanerolle NC. Loss of glutamine synthetase in the human epileptogenic hippocampus: possible mechanism for raised extracellular glutamate in mesial temporal lobe epilepsy. Lancet. 2004; 363:28–37. [PubMed: 14723991]
12. Eid T, Williamson A, Lee TS, Petroff OA, de Lanerolle NC. Glutamate and astrocytes – key players in human mesial temporal lobe epilepsy? Epilepsia. 2008; 49:42–52. [PubMed: 18226171]
13. Sepkuty JP, Cohen AS, Eccles C, Rafiq A, Behar K, Ganel R, Coulter DA, Rothstein JD. A neuronal glutamate transporter contributes to neurotransmitter GABA synthesis and epilepsy. J Neurosci. 2002; 22:6372–9. [PubMed: 12151515]

14. Robinson SR. Changes in the cellular distribution of glutamine synthetase in Alzheimer's disease. J Neurosci Res. 2001; 66:972–80. [PubMed: 11746426]
15. Tilleux S, Hermans E. Neuroinflammation and regulation of glial glutamate uptake in neurological disorders. J Neurosci Res. 2007; 85:2059–70. [PubMed: 17497670]
16. Seifert G, Schilling K, Steinhauser C. Astrocyte dysfunction in neurological disorders: a molecular perspective. Nat Rev Neurosci. 2006; 7:194–206. [PubMed: 16495941]
17. Pekny M, Nilsson M. Astrocyte activation and reactive gliosis. Glia. 2005; 50:427–34. [PubMed: 15846805]
18. Wilhelmsson U, Li L, Pekna M, Berthold CH, Blom S, Eliasson C, Renner O, Bushong E, Ellisman M, Morgan TE, Pekny M. Absence of glial fibrillary acidic protein and vimentin prevents hypertrophy of astrocytic processes and improves post-traumatic regeneration. J Neurosci. 2004; 26:5016–21. [PubMed: 15163694]
19. Wetherington J, Serrano G, Dingledine R. Astrocytes in the epileptic brain. Neuron. 2008; 58:168–78. [PubMed: 18439402]
20. Steffens M, Huppertz HJ, Zentner J, Chauzit E, Feuerstein TJ. Unchanged glutamine synthetase activity and increased NMDA receptor density in epileptic human neocortex: implications for the pathophysiology of epilepsy. Neurochem Int. 2005; 47:379–84. [PubMed: 16095760]
21. Rosati A, Marconi S, Pollo B, Tomassini A, Lovato L, Maderna E, Maier K, Schwartz A, Rizzuto N, Padovani A, Bonetti B. Epilepsy in glioblastoma multiforme: correlation with glutamine synthetase levels. J Neurooncol. 2009; 93:319–24. [PubMed: 19183851]
22. Barberis A, Petrini EM, Cherubini E. Presynaptic source of quantal size variability at GABAergic synapses in rat hippocampal neurons in culture. Eur J Neurosci. 2004; 20:1803–10. [PubMed: 15380001]
23. Parpura V, Basarsky TA, Liu F, Jeftinija K, Jeftinija S, Haydon PG. Glutamate-mediated astrocyte-neuron signalling. Nature. 1994; 30:744–7. [PubMed: 7911978]
24. Rizzoli SO, Betz WJ. Synaptic vesicle pools. Nat Rev Neurosci. 2005; 6:57–69. [PubMed: 15611727]
25. Burrone J, Li Z, Murthy VN. Studying vesicle cycling in presynaptic terminals using the genetically encoded probe synaptopHluorin. Nat Protoc. 2006; 1:2970–8. [PubMed: 17406557]
26. Oliva AA Jr, Jiang M, Lam T, Smith KL, Swann JW. Novel hippocampal interneuronal subtypes identified using transgenic mice that express green fluorescent protein in GABAergic interneurons. J Neurosci. 2000; 20:3354–68. [PubMed: 10777798]
27. Ang CW, Carlson GC, Coulter DA. Hippocampal CA1 circuitry dynamically gates direct cortical inputs preferentially at theta frequencies. J Neurosci. 2005; 19:9567–80. [PubMed: 16237162]
28. Ang CW, Carlson GC, Coulter DA. Massive and specific dysregulation of direct cortical input to the hippocampus in temporal lobe epilepsy. J Neurosci. 2006; 26:11850–6. [PubMed: 17108158]
29. Bushong EA, Martone ME, Jones YZ, Ellisman M. Protoplasmic astrocytes in CA1 stratum radiatum occupy separate anatomical domains. J Neurosci. 2002; 22:183–92. [PubMed: 11756501]
30. Mozrzymas JW, Wójtowicz T, Piast M, Lebida K, Wyrembek P, Mercik K. GABA transient sets the susceptibility of mIPSCs to modulation by benzodiazepine receptor agonists in rat hippocampal neurons. J Physiol. 2007; 585:29–46. [PubMed: 17855751]
31. Cohen AS, Lin DD, Coulter DA. Protracted postnatal development of inhibitory synaptic transmission in rat hippocampal area CA1 neurons. J Neurophysiol. 2000; 84:2465–76. [PubMed: 11067989]
32. Sun HY, Lyons SA, Dobrunz LE. Mechanisms of target-cell specific short-term plasticity at Schaffer collateral synapses onto interneurones versus pyramidal cells in juvenile rats. J Physiol. 2005; 568:815–40. [PubMed: 16109728]
33. Jakubs K, Bonde S, Iosif RE, Ekdahl CT, Kokaia Z, Kokaia M, Lindvall O. Inflammation regulates functional integration of neurons born in adult brain. J Neurosci. 2008; 28:12477–88. [PubMed: 19020040]
34. Galic MA, Riazi K, Heida JG, Mouihate A, Fournier NM, Spencer SJ, Kalynchuk LE, Teskey GC, Pittman QJ. Postnatal inflammation increases seizure susceptibility in adult rats. J Neurosci. 2008; 28:6904–13. [PubMed: 18596165]

35. Binder DK, Steinhauser C. Functional changes in astroglial cells in epilepsy. Glia. 2006; 54:358–68. [PubMed: 16886201]

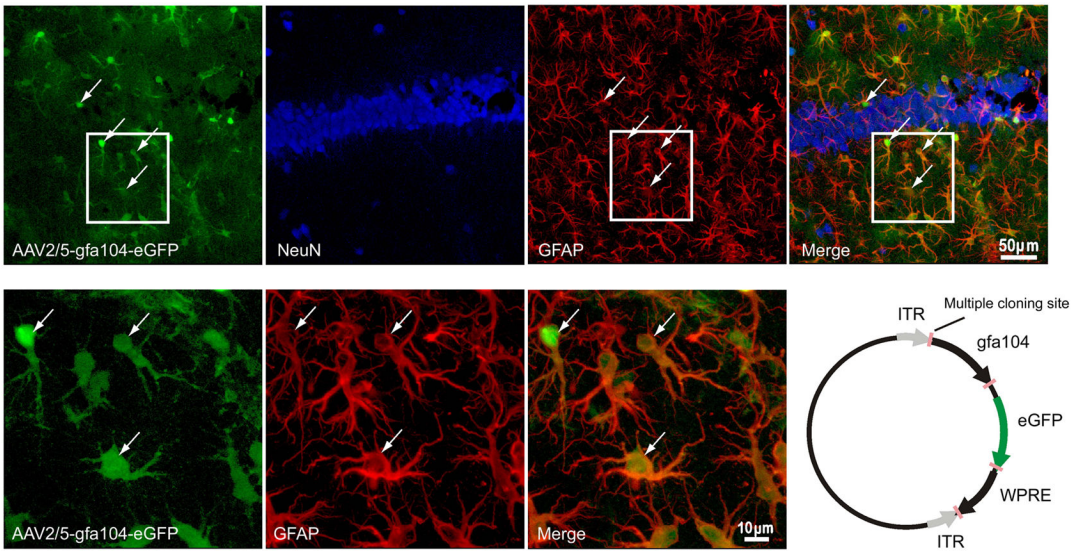

Figure 1. Astrocyte-specific eGFP expression

(**a–d**) Confocal images depicting (**a**) viral injection-induced eGFP expression (green), (**b**) immunostaining for NeuN (blue), and (**c**) GFAP (red) in the hippocampus. (**d**) eGFP co-localizes with GFAP (astrocyte marker; arrows) but not with NeuN (neuronal marker). (**e–g**) High magnification images show co-labeling of eGFP fluorescence with GFAP staining. (**h**) Schematic of the AAV2/5-gfa104-eGFP plasmid (see METHODS for details).

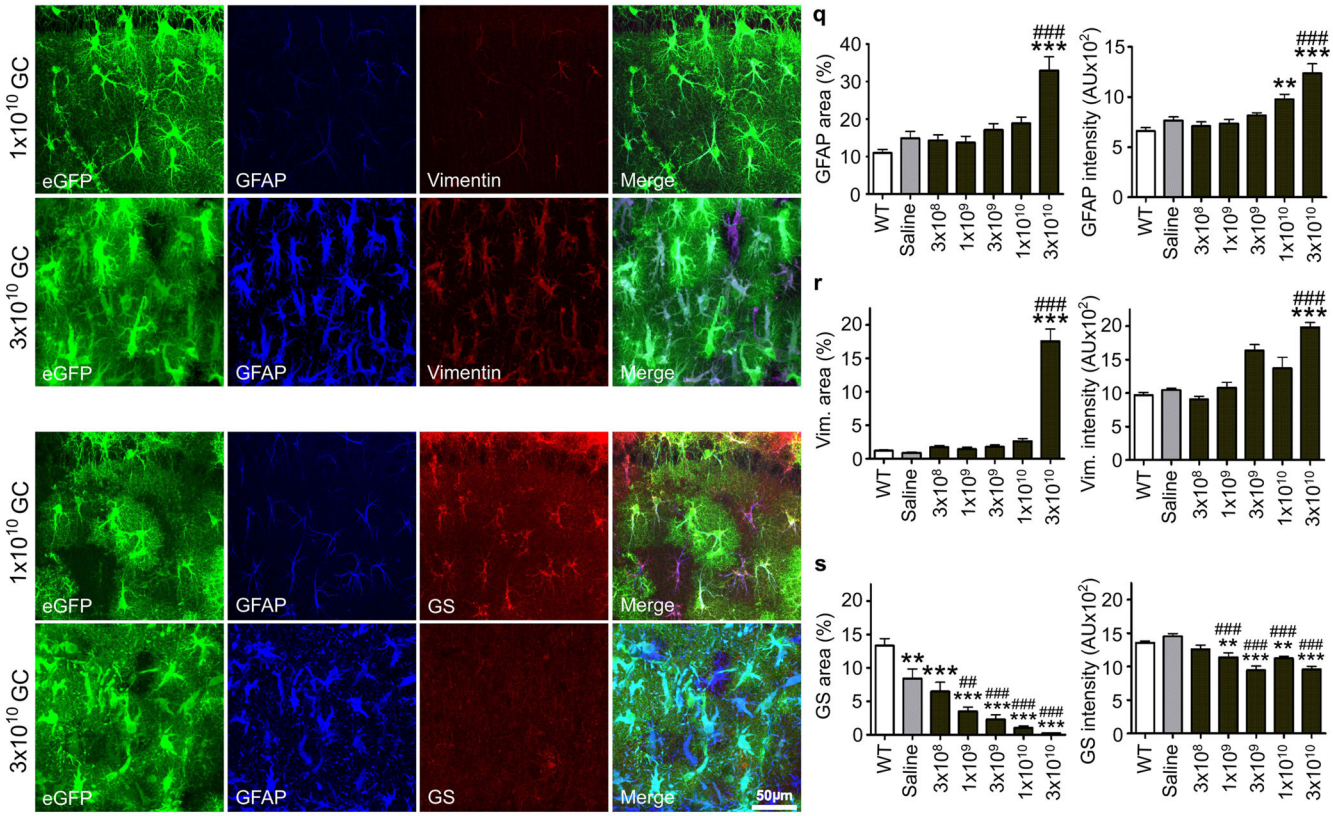

Figure 2. AAV2/5-gfa104-eGFP induces a titer-dependent reactivity of astrocytes

(**a–d**) Following low viral titer injection (1×10^9 GC/injection), $eGFP^+$ cells exhibit normal astrocytic morphology, and low levels of GFAP and vimentin staining. (**e–h**) In contrast, $eGFP^+$ cells labeled by high titer injection (3×10^{10} GC/injection) of the virus display a hypertrophic morphology typical of reactive astrocytes (**e**) and intense GFAP and vimentin staining (**f,g**). (**i–l**) Following low titer injection, $eGFP^+/GFAP^+$ cells show normal astrocytic morphology and are immunoreactive for glutamine synthetase, an astrocyte-specific enzyme. (**m–p**) High titer injection leads to a loss of glutamine synthetase immunoreactivity in $eGFP^+/GFAP^+$ cells. Merged images are shown in **d, h, l** and **p**. (**q–s**) Titer-dependence of GFAP, vimentin and glutamine synthetase immunostaining in the stratum radiatum. Expression levels were quantified as the area with immunoreactivity exceeding a background threshold intensity and as the average intensity of immunoreactivity. **, $p<0.01$; ***, $p < 0.001$, relative to wild-type animals. ##, $p<0.01$; ###, $p<0.001$, relative to saline-injected animals. Error bars, s.e.m.

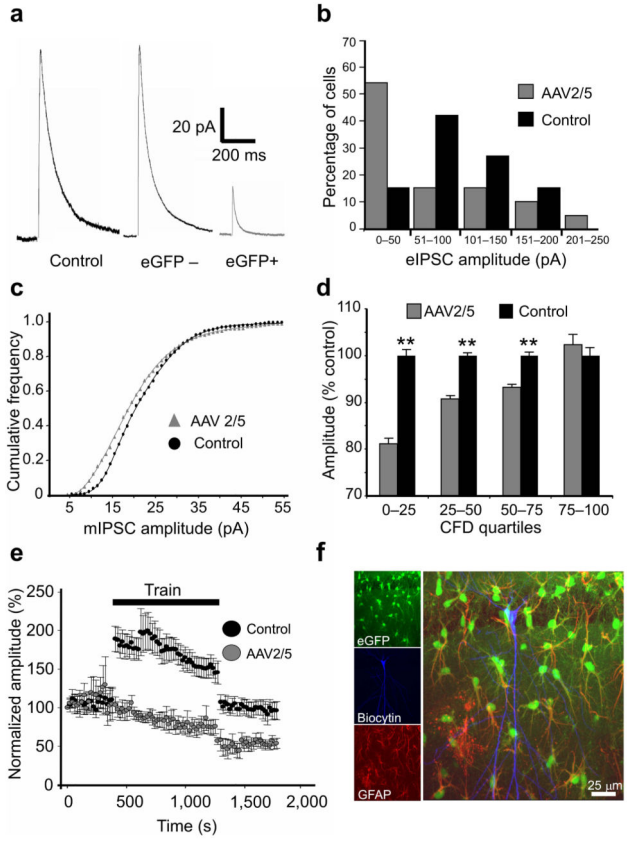

Figure 3. Inhibitory neurotransmission is impaired in CA1 pyramidal cells proximal to reactive astrocytes

(**a**) Sample traces of eIPSCs from control cells and pyramidal cells located distal (eGFP^{-}) and proximal (eGFP^{+}) to AAV2/5 transduced astrocytes. eIPSCs are much smaller in neurons neighboring reactive astrocytes (**b**) Histograms of eIPSC amplitude distribution in CA1 neurons of control and AAV2/5-injected animals. The IPSC distribution in eGFP^{+} neurons is skewed towards smaller values compared to controls. (**c**) Cumulative frequency distributions of mIPSC amplitudes from 4 AAV2/5 and 6 control cells. Note that the amplitude distribution is shifted to the left in AAV2/5 cells compared to controls and that small amplitude mIPSCs are maximally shifted (distributions significantly different, p=0.001, K-S test). (**d**) mIPSC amplitudes in AAV2/5 and control cells, grouped by quartile, are normalized to the mIPSC average in controls and compared. The degree of mIPSC reduction in AAV2/5 neurons gradually diminishes as the quartile increases in the population distribution (**, p<0.001, K-S test, error bars, s.e.m.). (**e**) Averaged time series of evoked responses before, during, and after the train stimulation (4 pulses at 50 Hz every 20 seconds for 15 minutes) in control and AAV2/5 cells, normalized to the amplitude of the first evoked event. Train stimulation elicits a long-term (persisting for at least the duration of recording, >8 minutes) depression of eIPSCs in cells from AAV2/5-injected, but not control animals. Error bars, s.e.m. (**f**) A representative CA1 pyramidal cell filled with biocytin (blue) surrounded by eGFP (green)/GFAP (red)-positive astrocytes.

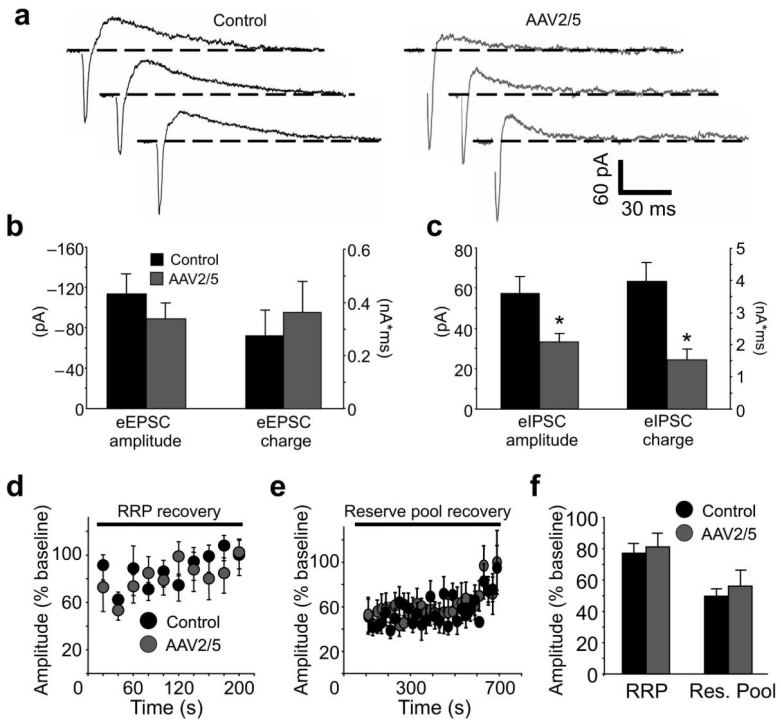

Figure 4. Preserved excitatory neurotransmission in CA1 pyramidal neurons proximal to reactive astrocytes

(**a**) Traces from a CA1 pyramidal cell in a control and an AAV2/5 slice recorded in the absence of glutamate and $GABA_A$ receptor antagonists (V_{hold}= −40 mV). An eIPSC follows an eEPSC in each trace. Note that EPSCs are similar in amplitude, while IPSCs are reduced. (**b,c**) Histograms of eEPSC and eIPSC amplitude and charge transfer. eEPSC amplitudes and charge transfers are similar (eEPSC amplitude: control n=10, AAV2/5 n=15, p=0.34; eEPSC charge: control n=9, AAV2/5 n=12, p= 0.59) while eIPSC amplitudes and charge transfer are both smaller in AAV2/5 cells (eIPSC amplitude: control n=6, AAV2/5 n=12, *, p=0.014; eIPSC charge: control n=6, AAV2/5 n=12, *, p=0.006). AAV2/5 eIPSC average excludes two cells that failed to exhibit an eIPSC at stimulation intensities used to elicit an excitatory response. (**d,e**) Time-course of eEPSC recovery from RRP (20 Hz, 2 s) and reserve pool (10 Hz, 90 s) stimulations. Amplitudes are normalized to the average (baseline) eEPSC during 10–15 single pulses (0.07 Hz) prior to RRP and reserve pool stimulation. (**f**) A histogram of average eEPSC amplitudes. eEPSCs were evoked at 0.07 Hz over a period of 5 minutes following RRP stimulation and 12 minutes following the reserve pool stimulation (control RRP n=9, reserve pool n=8, AAV2/5 RRP n=8, reserve pool n=7). Basal eEPSC current amplitudes were not different in the absence and presence of picrotoxin in either the control (p=0.1) or the AAV2/5 group (p=0.35). Error bars, s.e.m.

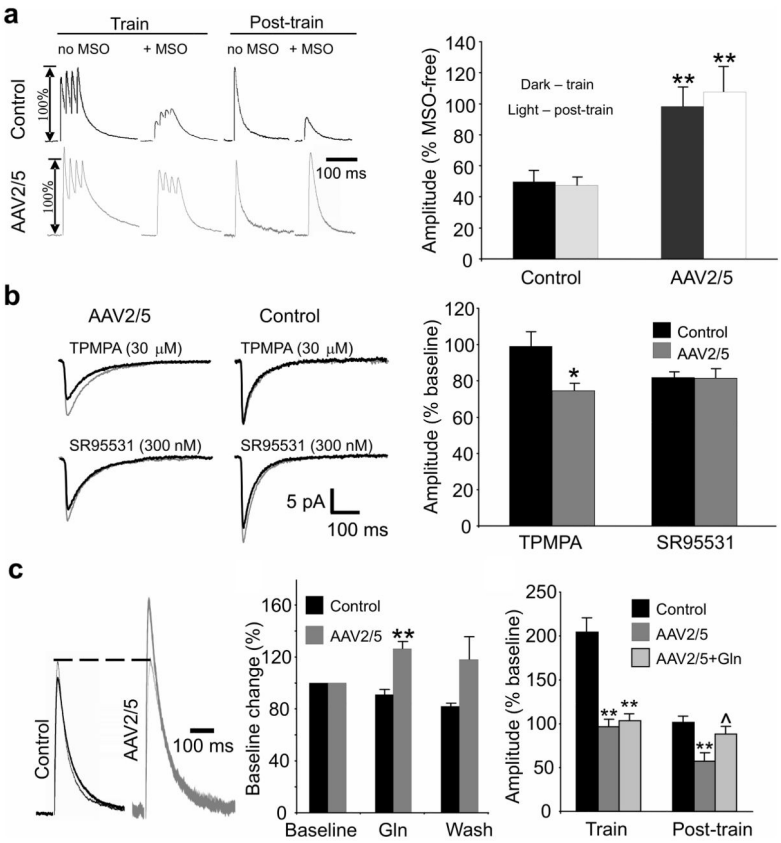

Figure 5. Glutamate-glutamine cycle deficits reduce concentration of vesicular GABA

(**a**) ***Left***, eIPSCs of MSO-treated cells compared to cells not exposed to MSO during and following train stimulation. ***Right***, Effect of train stimulation on eIPSC amplitudes following incubation in MSO (1.5 mM) is expressed as % change from eIPSCs recorded in the absence of MSO (c.f. Fig. 3e). MSO triggers an activity-dependent decrease of eIPSC amplitude in control, but not AAV2/5 cells (**, $p<0.001$ relative to control). (**b**) ***Left***, mIPSC averages in the absence (thin traces) and presence (thick traces) of TPMPA and SR95531. ***Right***, TPMPA significantly reduces mIPSC amplitude in neurons from AAV2/5 $eGFP^+$ cells (AAV2/5 (+/− TPMPA): 9.5±1.2 pA/7.1±0.9 pA, n=6, p=0.005, paired t-test; control (+/− TPMPA): 12.5±1.6 pA/12.2±2 pA, n=6, p=0.87, paired t-test). SR95531 reduces mIPSC amplitude to a similar extent in both groups of cells (AAV2/5 (+/− SR95531): 12.3±1.4 pA/9.9±1.4 pA, n=5, p=0.033, paired t-test; control (+/− SR95531): 13.6±2.1 pA/11.1±1.8 pA, p=0.004, paired t-test). *, p=0.027, compared to controls. (**c**) ***Left***, Current traces before (thin trace) and during (thick trace) application of 10 mM glutamine. ***Middle***, Supplementation with glutamine partially reverses eIPSC failure in a subset of AAV2/5 cells (**, $p<0.001$ relative to control; AAV2/5 n=5, control n=7). ***Right***, Bath-applied glutamine restores eIPSC amplitudes to control levels following train stimulation, but fails to prevent the eIPSC failure during the train (**, $p\leq0.003$ relative to control, ^, p=0.04 relative to AAV2/5). Cell numbers (train/post-train) are as follows: control n=12/10, AAV2/5 n=10/6, AAV2/5+Gln n=6/5. Error bars, s.e.m.

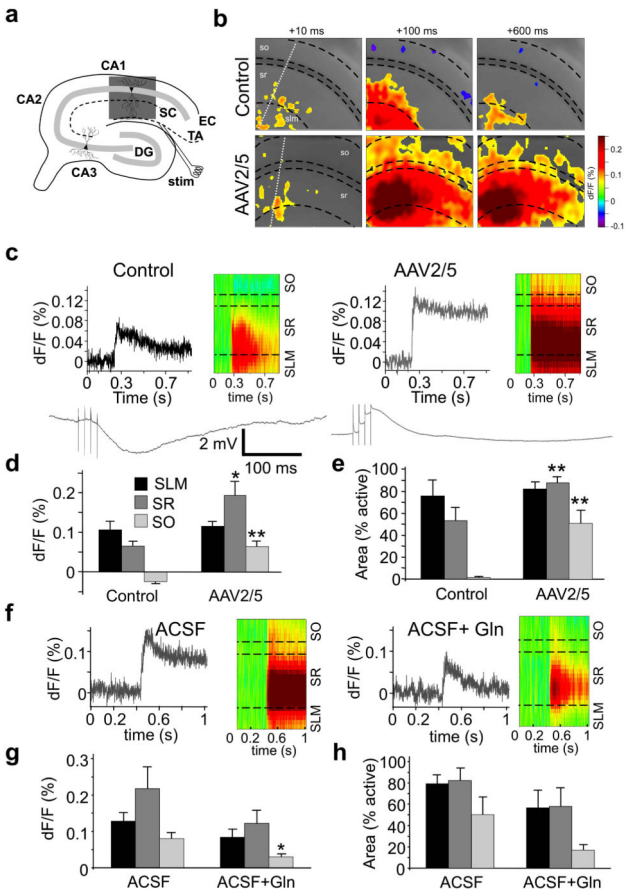

Figure 6. Reactive gliosis is associated with network hyperexcitability

(**a**) A hippocampal preparation schematic. Shaded box represents an area used for snapshots in (b). DG, dentate gyrus; EC, entorhinal cortex; stim, stimulation electrode. (**b**) VSD signal snapshots at indicated time points following onset of the TAP stimulus. White dotted lines indicate the pixels sampled for Raster plots in (c) SLM, *stratum lacunosum moleculare*, SR, *stratum radiatum*, SO, *stratum oriens*. (**c**) ***top row,*** Amplitude and time-course of the fluorescent signal and a Raster plot of hippocampal activity across the CA cell layers. Note compartmentalization of the EPSP to distal SR in the control, but not the AAV2/5 slice. ***bottom row,*** Current-clamp traces from CA1 pyramidal neurons. TAP stimulation elicits an EPSP in cells from AAV2/5 eGFP$^+$ areas and an IPSP in cells from control animals. (**d,e**) Amplitude of the fluorescent signal and area activated by TAP stimulation (** $p<0.008$, * $p=0.016$; control n=6, AAV2/5 n=10). An SO IPSP in the control slices converts to an SO EPSP in slices from eGFP$^+$ AAV2/5 slices. (**f**) Fluorescence changes triggered by TAP activation before (*Left*) and following (*Right*) a 15-minute bath-application of glutamine to an eGFP$^+$ AAV2/5 slice. (**g,h**) Normalized fluorescence change and activated area before and after glutamine application in AAV2/5 eGFP$^+$ slices (*, $p=0.04$, paired t-test, n=5). In SO, the active area is smaller in the AAV2/5 group, but fails to reach significance relative to the control group ($p=0.09$, paired t-test). Error bars, s.e.m.